Unusual Rheological Characteristics of Polypropylene/Organoclay Nanocomposites in Continuous Cooling Process

Xi Fan, Zhicheng Wang, Ke Wang, Hua Deng, Feng Chen, Qiang Fu

Department of Polymer Science and Materials, State Key Laboratory of Polymer Materials Engineering, Sichuan University, Chengdu 610065, People's Republic of China

Received 12 August 2010; accepted 1 December 2010
DOI 10.1002/app.36401
Published online 15 January 2012 in Wiley Online Library (wileyonlinelibrary.com).

ABSTRACT: The cooling process of isotactic polypropylene (iPP)/organoclay nanocomposites was followed by dynamic rheometry. Contrasting to typical linear increment of log G' with decreasing temperature (log $G' \propto 1/T$) occurred on the melts for neat iPP and nanocomposites with small amounts of organoclay, an unusual rheological behavior was identified for composites with relative high organoclay content ($\geq$5 wt %) as that: increasing of log G' positively deviates to linear relation during cooling within certain high temperature region, thus yields an additional enhancement in viscoelastic properties. Furthermore, such unusual rheological phenomenon was found to be strongly impacted by initial dispersion level of organoclay, cooling rate, and construction of organoclay network. The origin of this unusual rheological phenomenon could be cautiously explained as due to the existence of unstable state of organoclay nanostructure, which could go further intercalation or exfoliation in some high temperature ranges. This might be a new rheological character and is meaningful for understanding the essentially structural behavior of polymer/layered clay nanocomposites, particularly containing mesoscopic clay network. © 2012 Wiley Periodicals, Inc. J Appl Polym Sci 125: E292–E297, 2012

Key words: unusual rheological behavior; polymer/clay nanocomposite; cooling process

INTRODUCTION

Polymer/clay nanocomposites (PCNs) have attained extensive attention in the past decade, due to remarkable enhancements in physical and/or chemical properties.[1–3] Obviously, macroscopic performances are highly dependent on nanoscale structure of layered clay, typically such as intercalated and exfoliated structure. To explore the essential features of clay nanoscale structure in PCNs, melt rheometry has been frequently utilized in previous literature[4–9] to assess various physical aspects like dispersed state,[4] percolated clay network,[5] orientation/relaxation,[6] confinement effect,[7] transient structural/morphological change,[8] interaction between polymer and clay,[9] etc. Among these research subjects, the aspect of transient structural/morphological change is notable and highly relevant in this study.

Even under quiescent molten conditions (undisturbed by external shear fields), the dispersion state of clay nanoparticles in PSNs melt is variable because molten polymer chains with high mobility tend to further diffuse and intercalate into intergallery between clay layers, resulting in an higher level of intercalation/exfoliation and more uniform dispersion. Rheologically affirming the unstable state of clay nanostructure was first performed by Lim and Park,[10] in their study the storage modulus of polystyrene/organoclay nanocomposite melt was improved continuously with increasing annealing time. As to nonpolar polymer matrix, for example, polypropylene, the kinetics of changes in clay dispersion was relative slow, but, interestingly, after certain long waiting duration a gel-like rheological character appeared in the logarithmical relation between storage modulus and annealing time.[11,12] Spontak and coworkers[13] suggested that the phenomenon of self-occurred intercalation/exfoliation under quiescent molten condition can be utilized as a facile route to attain well-dispersed PCNs. However, in past literature, the rheological investigations about structural alteration of PSNs melt were almost implemented upon isothermal situation, whereas the variable temperature process was rarely concerned.[14] Obviously, the latter process is highly relevant to practical processing fabrication of PCNs materials and is valuable for investigating in detail.

In this article, the continuously cooling event of isotactic polypropylene/organoclay nanocomposite melts was inspected by dynamic rheometry. The main objective was to illustrate the rheological

Correspondence to: K. Wang (wkestar@scu.edu.cn) or Q. Fu (qiangfu@scu.edu.cn).

Contract grant sponsor: National Natural Science Foundation of China; contract grant numbers: 50973065, 50873063, 20874064.

characteristics of cooling process of nanocomposite melt, thus distinguish the mechanism of transient structural change occurred in such process, taking account into the presence of nanoscale organoclay platelets and especially the formation of mesoscopic organoclay network.

EXPERIMENTAL

Materials

A commercially available isotactic polypropylene (trade marked as T30S, Yan Shan Petroleum, China) with a melt flow index (MFI) of 2.64 g/10 min (210°C, 2.16 kg loading), $M_w = 39.9 \times 10^4$ g/mol and $M_w/M_n = 4.6$, and a maleic anhydride-grafted polypropylene (PP-*g*-MA) with maleic anhydride (MA) content = 0.9 wt %, MFI = 6.74 g/10 min, $M_w = 21.1 \times 10^4$ g/mol, and $M_w/M_n = 3.2$ were used as the base polymers. Southern Clay Products provided Cloisite 15A (125 mequiv/100 g, $d_{001} = 31.5$ Å), a natural MMT clay modified with a ditallow quaternary ammonium salt (2M2HT).

Preparation of composites

Master-batch pellets with a composition of iPP/PP-*g*-MA/Cloisite 15A (70/15/15 wt %) were first melt-mixed in a TSSJ-2S corotating twin-screw extruder. The temperature of the extruder was maintained at 170°C, 180°C, 190°C, 200°C, 200°C, and 195°C from hopper to die, and the screw speed was about 120 rev/min. Then a series of iPP/PP-*g*-MA/Cloisite 15A nanocomposite (90/10/x wt %, x =1, 3, 5, 7, 9) were obtained through adding iPP and PP-*g*-MA to dilute the as-prepared master-batch in the extruder. The resulted nanocomposite is hereafter abbreviated as PPCNx (x = 1, 3, 5, 7, and 9, represented the mass content of organoclay). An unfilled iPP/PP-*g*-MA (90/10 wt %) blend was also prepared for comparison and is denoted as PPCN0.

Characterizations

Wide-angle X-ray diffraction

WAXD analysis was conducted on a DX-100 X-ray diffractometer (radiation Cu Kα, λ = 0.154 nm, reflection mode). The 2θ range was 2°–10° with a scanning rate of 0.02°/s.

Melt rheometry

The rheological measurements were performed on controlled stress rheometer (Malvern Instruments Ltd., UK) using 2.5 cm diameter parallel plates. Testing sample disks with a thickness of 1.5 mm and a diameter of 2.5 mm were prepared by compression molding of the extruded pellets at 190°C for 3 min. Three procedures of rheological measurement were carried out: (i) small-amplitude oscillatory shear (SAOS) mode at 190°C, upon constant stress = 10 Pa and within a frequency range of 0.03–100 rad/s; (ii) dynamic temperature sweep mode upon isochronal conditions, i.e., the storage modulus (G') was measured at a fixed angular frequency (ω) of 0.1 rad/s and under constant stress = 10 Pa, during the decreased temperature processes from 210°C to 125°C with cooling rates of 1.5, 2.5, and 5°C/min; (iii) a steady step-shear (shear rate = 2 s^{-1}) was exerted on the testing melts under 210°C for an interval of 300 s, then followed by the procedure (ii).

RESULTS AND DISCUSSION

The cooling processes of the basal iPP resin and nanocomposites with different organoclay contents have been followed through monitoring the development of rheological properties (storage and loss moduli) with decreasing temperature upon a cooling rate of 1.5°C/min, which are plotted as Figure 1. It should be noted that the evolution trend of storage modulus is almost same to that of loss modulus, thus only storage modulus is mentioned. Typical Arrhenius behavior is observed for the melts of PPCN0, PPCN1, and PPCN3. Good linear relation between log G' and temperature that log G' is improved monotonically with continuously decreasing of temperature is maintained almost within the entire measured-temperature range until an abrupt increment occurred at about 128°C, which relates to significant liquid-to-solid transition of primary nucleation and crystallization. When the organoclay content is high as 5, 7, and 9%, the dependence of log G' on temperature before the occurrence of primary crystallization is nonlinear and becomes more complicated, comparing to the nanocomposites with low contents of organoclay. Within certain high temperature regime, the development of log G' positively deviates to linear relation with temperature, and thus induces an additional enhancement in rheological property. After experiencing the nonlinearly enhanced regime, the relation between log G' and temperature regresses to typical Arrhenius behavior until the beginning of primary crystallization. Interestingly, the raised amplitude and temperature range of the nonlinearly enhanced regime for log G' is dependent obviously on the organoclay content. The higher the organoclay content, the stronger the raised amplitude as well as the broader the temperature range. It is logically deduced that there exists a structurally unstable state in high temperature regime of cooling process of nanocomposite melts with large amounts of organoclay.

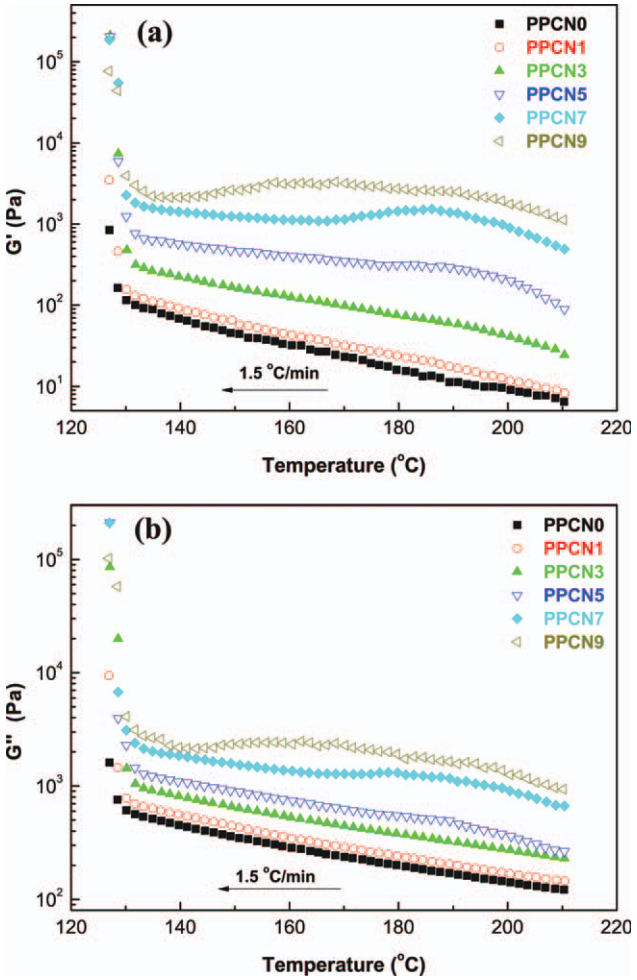

Figure 1 Isochronal dynamic temperature sweep experiments at ω = 0.1 rad/s and cooling rate equals to 1.5°C/min. The variations of storage modulus (a) and loss modulus (b) with temperature for the matrix polymer and prepared nanocomposites. [Color figure can be viewed in the online issue, which is available at wileyonlinelibrary.com.]

To reveal the origin of the unusual rheological behavior described above, the development of rheological properties (storage and loss moduli) with decreasing temperature has been followed upon three different cooling rates (1.5, 2.5, and 5°C/min) for PPCN5, PPCN7, and PPCN9. Representatively, the effect of cooling rate on rheological behavior during cooling process of PPCN9 is illustrated in Figure 2. The temperature range of the nonlinearly enhanced regime is reduced remarkably and the raised amplitude of nonlinearly enhanced regime is also depressed as increasing the cooling rate from 1.5°C/min to 2.5°C/min, whereas the dependence of log G' on temperature is accordant with linear relation of Arrhenius behavior when the cooling rate is high as 5°C/min. As to PPCN5 and PPCN7, similar phenomenon has been seen (not shown here). For molten polymer/organoclay systems, the dispersion state of organoclay nanoparticles is variable upon quiescent condition, and the polymer chains with high mobility commonly tend to further diffuse and intercalate into intergallery of organoclay stacks, thus results in higher level of intercalation and exfoliation. This behavior of transient structural change has been affirmed by *in situ* measurements of isothermal melt rheometry[11] and time-resolved WAXD analysis.[15]

The structural change of organoclay dispersion in PPCN9 after cooling upon different cooling rates has been assessed by WAXD, and the corresponding XRD patterns are shown in Figure 3. For a clarity purpose, the corresponding peak maxima of (001) plane and *d*-spacings of organoclay are listed in Table I. For low cooling rate of 1.5°C/min, the diffraction peak of orderly stacking platelets becomes feint and broadens, indicating a further intercalation and exfoliation during this cooling process. Whereas, obvious diffraction peaks of (001) plane still reserve

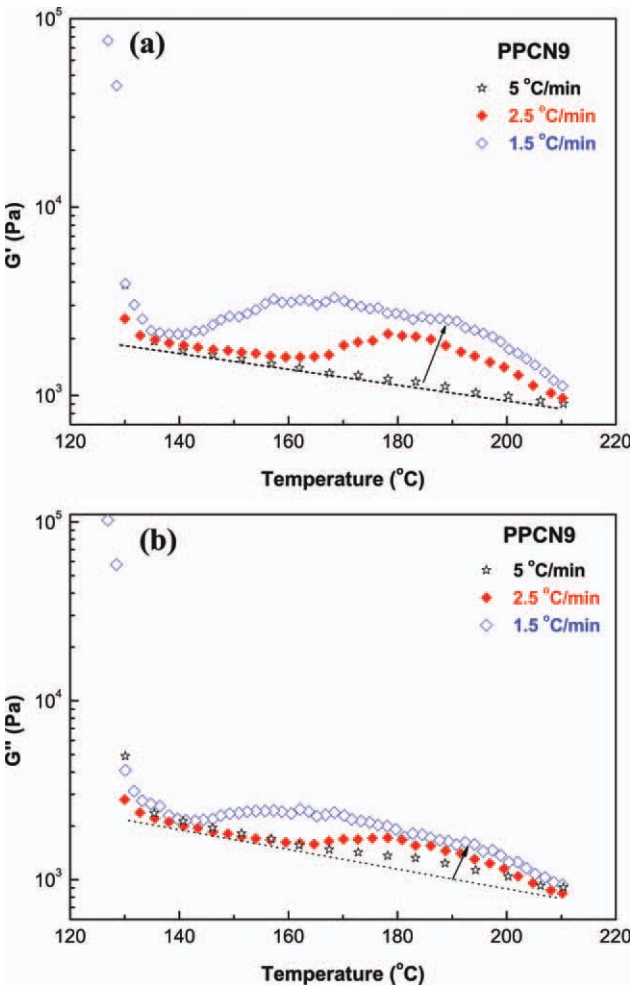

Figure 2 Variations of storage modulus (a) and loss modulus (b) with temperature during isochronal dynamic temperature sweep experiments at ω = 0.1 rad/s for the PPCN9. Cooling rate: (◇) 1.5°C/min, (♦) 2.5°C/min, and (☆) 5.0°C/min. [Color figure can be viewed in the online issue, which is available at wileyonlinelibrary.com.]

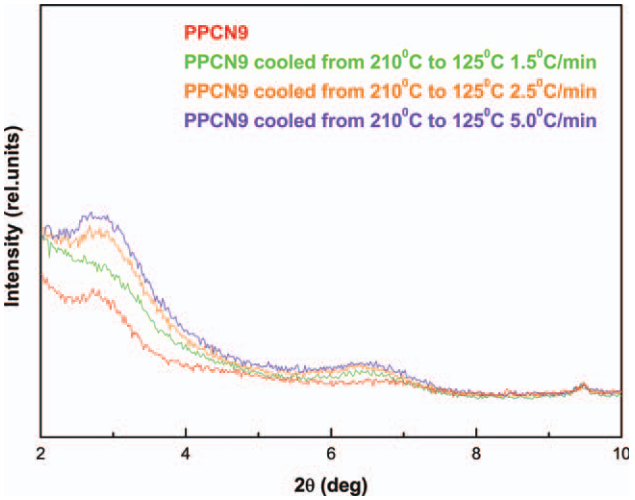

Figure 3 XRD pattern of PPCN9 after cooling from 210°C to 125°C with various cooling rate. [Color figure can be viewed in the online issue, which is available at wileyonlinelibrary.com.]

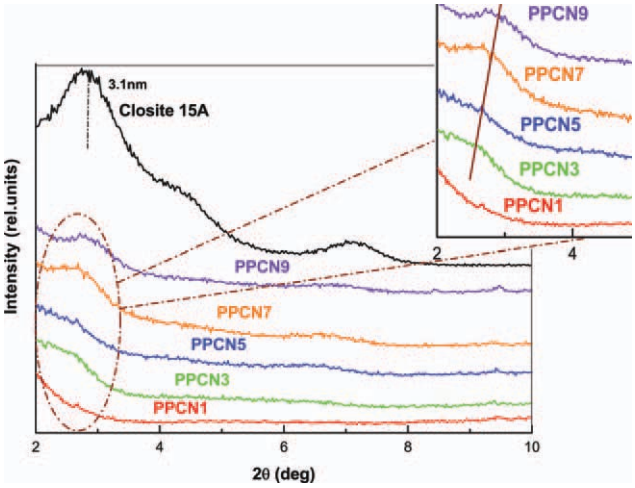

Figure 4 XRD pattern of Cloisite 15A and PCNs with different clay concentrations. An enlarged region of organoclay (001) plane in nanocomposite is presented as inset. [Color figure can be viewed in the online issue, which is available at wileyonlinelibrary.com.]

after the cooling processes upon fast cooling rates of 2.5 and 5°C/min, this suggests that the dispersion state of organoclay dose not change much in these two processes. Therefore, the origin of the nonlinearly enhanced log G' with temperature within high temperature regime can be due to the existence of unstable state of organoclay nanostructure, which could go further intercalation or exfoliation in some high temperature ranges, just in a case of high temperature annealing, leading to an additional enhancement in rheological property. This additionally enhanced effect forces the development of log G' to deviate from the linear relation with temperature derived merely by the effect of decreasing of temperature. If the cooling rate is fast, there is no enough time for dispersion state of organoclay nanoparticles develops significantly, thus the nonlinear enhancement of log G' within high temperature regime cannot appear.

Once the reason of the appearance of such unusual rheological behavior is revealed, it is logical to ask why this phenomenon occurs mainly for the nanocomposites with high contents of organoclay and becomes obvious as increasing of organoclay content. The initial dispersion situation of organoclay in iPP basal resin before rheological experiment has been estimated by WAXD analysis, and the XRD patterns corresponded to the original Cloisite 15A and nanocomposites with different organoclay contents are presented in Figure 4. Moreover, the corresponding peak maxima of (001) plane and *d*-spacings of organoclay are listed in Table II. According to the (001) peak at 2.9°, the interspacing between organoclay platelets (*d*-spacing) of Cloisite 15A is calculated as 3.1 nm by the Bragg equation. As to the nanocomposites, the dispersion situation of organoclay is dependent on the content of adding nanoparticles. The characteristic peaks of clay platelets stacking are unvisual when the organoclay content is low as 1%. Within the clay content range from 3 to 7%, the (001) peak shifts to lower 2θ, comparing to the original Cloisite 15A, indicating the intercalated organoclay stacks with *d*-spacing about 3.6 nm. When the clay content increases to 9%, the (001) peak correlated to *d*-spacing of 3.2 nm is detectable. Less amounts of unintercalated organoclay stack are reserved in PPCN9. Therefore, the intercalation/exfoliation level becomes bad with increasing the organoclay content. For the nanocomposites with low contents of organoclay, the initial situation of intercalation/exfoliation is good, and the nanostructure of organoclay alters faintly within cooling temperature process, thus the rheological property is almost undisturbed. Whereas, at high content range, since the initial level of intercalation/exfoliation is relatively low, the variable extent of organoclay structure during cooling process is large, resulting in a prominent effect of structure change of nanoparticles on the rheological behavior. Obviously, this effect is stronger at higher organoclay content. At current research stage, the extent of intercalation/exfoliation of organoclay is adjusted only by changing the nanoparticle content. In our future study, the

TABLE I
Maxima of (001) Peaks of Organoclay and Corresponding *d*-Spacings in Figure 3

	PPCN9	1.5°C/min	2.5°C/min	5°C/min
Peak maximum	1450	1259	1550	1666
d-spacing (nm)	3.15	3.5	3.19	3.17

TABLE II
Maxima of (001) Peaks of Organoclay and Corresponding *d*-Spacings in Figure 4

	Cloisite 15A	PPCN1	PPCN3	PPCN5	PPCN7	PPCN9
Peak maximum	3822	1145	1523	1577	1814	1450
d-spacing (nm)	3.08	–	3.72	3.62	3.56	3.15

organoclay content will be fixed at, such as, 9%, and the dispersion status of nanoparticles is modulated by varying compatibilizer (PP-*g*-MA) concentration and using different types of organically modified agent (intercalatant), to ascertain the effect of initial dispersion extent of organoclay on such observed unusual rheological behavior systematically.

As demonstrated extensively in previous literature,[16,17] the confinement of clay nanoparticles on the mobility of polymer chains may become stronger and stronger with increasing nanoparticle content, and when the nanoparticle content reaches certain critical value clay nanoparticles can establish mesoscopic, mechanically percolated network superstructure. The formation of clay network in polymer resin can be estimated qualitatively by the rheological testing of frequency sweep upon small-amplitude oscillatory shear (SAOS) mode. For the nanocomposites prepared in this study, the double-logarithmical curves of storage modulus (G') versus frequency (ω) are shown in Figure 5. The values of G' within the entire ω range are improved higher and higher with increasing the organoclay content (except the G' of PPCN9 within high ω regime is lower than that of PPCN7, because some unintercalated clay stacks are existed in PPSN9 as validated by WAXD). More importantly, the slope of log G'/log ω within low ω regime decreases continuously with increasing of organoclay content, indicating a change in melt rheological feature. For PPCN0, the log G' versus log ω slope within low ω regime (0.1–0.03 rad/s) is 1.18. The dependence of G' on ω within low ω regime becomes more and more weaken as the addition of organoclay, indicating a rheological transition from liquid-like behavior to pseudo-solid-like behavior.[18] The appearance of pseudo-solid-like behavior can be attributed to the formation of mesoscopic structure of percolated organoclay network at relative high nanoparticle content, which induces the significant enhancement in rheological properties. Additionally, it should be noted that the terminated slope of log G'/log ω varies significantly between PPCN5 and PPCN3 (as illustrated by the insert of Fig. 5), suggesting that the nanoparticle content threshold for the formation of mesoscopic, percolated organoclay network is at 5%.

Interestingly, as seen from Figure 1, the beginning content of organoclay for the appearance of the nonlinearly enhanced regime is also at 5%. Meanwhile, the profile character of such special regime is impacted remarkably by the complete degree of mesoscopic network structure (increasing organoclay content). So, the formation of organoclay network might play important role on this unusual rheological behavior. To destroy the percolated organoclay network formed in the nanocomposites containing high clay contents ($\geq$5%), the controlled steady preshear was imposed on the melts of nanocomposite. Subsequently, the development of log G' during the decreased temperature process upon cooling rate of 1.5°C/min was monitored again by rheometry. The resultant rheological spectra of log G' versus temperature are plotted in Figure 6 for the iPP basal resin and nanocomposites. For all of the melts, the G' within entire temperature range decreases prominently after experiencing the preshear treatment, indicating a structural transition from isotropy to anisotropy. It can be seen that, the percolated organoclay network, in which layered platelets and/or stacks randomly align along different directions, cannot be maintained for highly oriented texture. The unusual rheological behavior that the nonlinearly enhanced log G' within high temperature regime is extremely depressed after experiencing the preshear, even for composites with organoclay content as high as 9%. In the melts of PPCN5, PPCN7, and PPCN9, the log G' rapidly increases only within

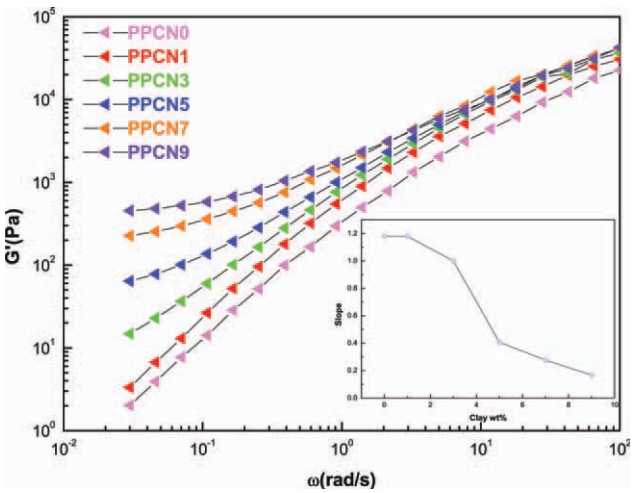

Figure 5 Plots of storage modulus (G') versus angular frequency for small amplitude oscillatory shear (SAOS) sweeps performed at 190°C. Data are reported for the matrix polymer and prepared nanocomposites. [Color figure can be viewed in the online issue, which is available at wileyonlinelibrary.com.]

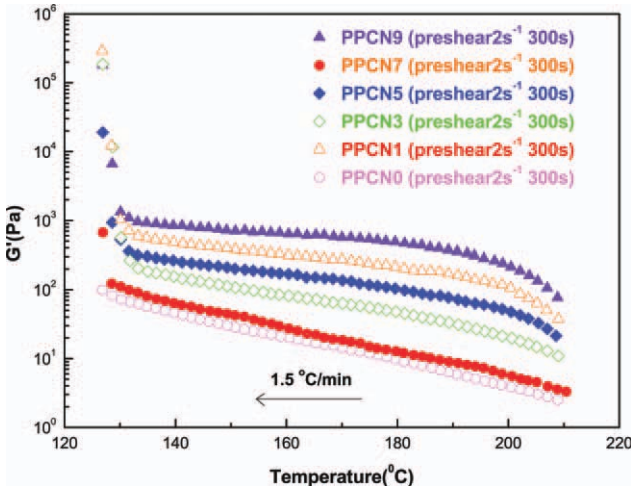

Figure 6 Isochronal dynamic temperature sweeps (cooling rate: 1.5°C/min) after steady shear deformation (shear rate = 2 s^{-1}) at an interval of 300 s. [Color figure can be viewed in the online issue, which is available at wileyonlinelibrary.com.]

very narrow range of high temperature, subsequently, the development of log G' with temperature exhibits as linear Arrhenius behavior. The self-occurred intercalation and exfoliation of organoclay stacks yielded upon quiescent molten condition as demonstrated above has been largely restricted in a molten orientation system. So, the absence of the nonlinearly enhanced regime in Figure 6 can be attributed to the destruction of percolated organoclay network. It can be envisaged that the enhanced effect derived from structural change of organoclay dispersion is more effective for an isotropic, percolated organoclay network than for an anisotropic, orientation texture of organoclay platelets and/or stacks. The formation of percolated organoclay network is the preliminary requirement for the appearance of the unusual rheological behavior demonstrated in this study. While the exhaustive explanation of the essential physics behind the apparent rheological phenomena needs be further investigated in future.

CONCLUSIONS

The rheological behavior of iPP/organoclay nanocomposite containing clay network dramatically differs to that of neat iPP resin and nanocomposite with low content of nanoparticle. Contrasting to the traditional Arrhenius behavior that linear relation between rheological property and temperature maintains within entire cooling process, the positive deviation of linear relation between G' and temperature has been indeed affirmed for nanocomposite melt with relative high content of organoclay, which results in an additional enhancement in viscoelastic properties within certain high temperature range. Although this unusual rheological behavior is directly due to the existence of unstable stage of organoclay dispersion, the formation of mesoscopic, percolated organocaly network plays the dominant role for the appearance of such rheological characteristics. It might be a newly found criterion for rheological behavior of PCNs containing nanoparticles network.

References

1. Fornes, T. D.; Hunter, D. L.; Paul, D. R. Macromolecules 2004, 37, 1793.
2. Rao, Y. Q.; Pochan, J. M. Macromolecules 2007, 40, 290.
3. Zax, D. B.; Yang, D. K.; Santos, R. A.; Hegemann, H.; Giannelis, E. P.; Manias, E. J Chem Phys 2000, 112, 2945.
4. Durmus, A.; Kasgoz, A.; Macosko, C. W. Polymer 2007, 48, 4492.
5. Solomon, M. J.; Almusallam, A. S.; Seefeldt, K. F.; Somwangthanaroj, A.; Varadan, P. Macromolecules 2001, 34, 1864.
6. Ren, J. X.; Casanueva, B. F.; Mitchell, C. A.; Krishnamoorti, R. Macromolecules 2003, 36, 4188.
7. Muenstedt, H.; Katsikis, N.; Kaschta, J. Macromolecules 2008, 41, 9777.
8. Wang, K.; Hou, Z.-C.; Zhao, P.; Deng, J.-N.; Zhang, Q.; Fu, Q.; Dong, X.; Wang, D.-J.; Han, C.-C. J Chem Phys 2007, 127, 084901.
9. Manitiu, M.; Horsch, S.; Gulari, E.; Kannan, R. M. Polymer 2009, 50, 3786.
10. Lim, Y. T.; Park, O. O. Macromol Rapid Commun 2000, 21, 231.
11. Treece, M. A.; Oberhauser, J. P. Polymer 2007, 48, 1083.
12. Treece, M. A.; Oberhauser, J. P. Macromolecules 2007, 40, 571.
13. Frankowski, D. J.; Khan, S. A.; Spontak, R. J Adv Mater 2007, 19, 1286.
14. Mitchell, C. A.; Krishnamoorti, R. J Polym Sci Part B: Polym Phys 2002, 40, 1434.
15. Galgali, G.; Ramesh, C.; Lele, A. Macromolecules 2001, 34, 852.
16. Ren, J. X.; Silva, A. S.; Krishnamoorti, R. Macromolecules 2000, 33, 3739.
17. Wang, K.; Liang, S.; Deng, J.-N.; Yang, H.; Zhang, Q.; Fu, Q.; Dong, X.; Wang, D.-J.; Han, C.-C. Polymer 2006, 47, 7131.
18. Suh, C. H.; White, J. L. J Non-Newtonian Fluid Mech 1996, 62, 175.